Journal of Alloys and Compounds 488 (2009) 190–194

Contents lists available at ScienceDirect

Journal of Alloys and Compounds

journal homepage: www.elsevier.com/locate/jallcom

Enhancing nanoscale patterning on Ge–Sb–Sn–O inorganic resist film by introducing oxygen during blue laser-induced thermal lithography

Chung Ping Liu [a,*], Che Chuan Hsu [a], Tsun Ren Jeng [b], Jung Po Chen [b]

[a] Department of Photonics Engineering, Yuan Ze University, 135 Yuan Tung Rd., Chungli, Taoyuan 320, Taiwan, ROC
[b] Electronics and Optoelectronics Research Laboratories, ITRI, Hsinchu 300, Taiwan, ROC

ARTICLE INFO

Article history:
Received 21 May 2009
Received in revised form 15 August 2009
Accepted 17 August 2009
Available online 25 August 2009

Keywords:
Inorganic materials
Nanofabrications
Microstructure

ABSTRACT

This work describes a new inorganic resist material Ge–Sb–Sn–O (GSSO) for nanoscale patterning by thermal lithography in which a laser beam directly illuminates the resist film. The heat from the illuminating laser can change the phase of a resist material from amorphous to crystalline. During development, the contrast between the dissolution rates of these two states can cause the formation of nanoscale patterns. Experimental results demonstrate that nanoscale patterning on GSSO inorganic resist film can be improved by introducing oxygen into the film during blue laser-induced thermal lithography, and that the GSSO resist is positive. Additionally, when the numerical aperture is 0.65 and the wavelength is 405 nm, a minimum pattern width of 140 nm on the GSSO film and a height of 80 nm, far below the diffraction limit of 320 nm, can be obtained.

© 2009 Elsevier B.V. All rights reserved.

1. Introduction

Thermal lithography is adopted extensively for nanoscale patterning [1,2]. Although conventional optical lithography can utilize light of a shorter wavelength [3] or an electron beam [4] to reduce the size of pattern structure, it requires large and expensive facilities and is limited by the limit of diffraction. However, thermal lithography in which a laser beam is applied to illuminate directly a resist film is not limited by any diffraction limit and the facilities required are relatively simple. The cross-sectional light intensity profile within the focused laser spot has an approximate Gaussian distribution, which enables the formation of the hottest area that is smaller than the focused laser spot [5]. The heat from laser beam can alter the phase of the resist material from amorphous to crystalline. A crystalline state can be obtained by etching with alkaline or acid solution more easily than can an amorphous state [6]. The development process can yield nanoscale structures. Accordingly, since neither a particular light source nor a particular environment is necessary, thermal lithography is a low-cost and time-saving fabrication approach.

In recent years, various inorganic resist materials, including phase-changing materials, Te–O or Sb–O, and metal oxides, W–O or Mo–O, have been developed [6–8]. Inorganic resists are preferred because the molecular weight of an organic resist exceeds that of an inorganic resist and so its boundary between unexposed and exposed areas is unclear after laser heating [8]. Furthermore, the rate of increase of temperature of an inorganic resist exceeds that of an organic resist for a given irradiance. Therefore, inorganic resist is a good absorber of laser illumination in nanoscale patterning [9].

Although Ge–Sb–Sn (GSS) inorganic resist material has also been formed by thermal lithography, the rate of dissolution of exposed areas on GSS material is only 2.3 nm per minute [10]. Based on the authors' earlier work [2,11,12], the properties of such a film can be improved by introducing oxygen into it to increase the dissolution rate. In this study, two sputtering targets are adopted to deposit a new inorganic resist film Ge–Sb–Sn–O (GSSO) with the introduction of oxygen to narrow the nanoscale pattern obtained by thermal lithography.

2. Experimental

2.1. Preparation of sample

The sample has a multilayered structure, as shown in Fig. 1. The pitch width between the land and the groove on the surface of an optical disk substrate made of polycarbonate was 0.74 μm. A ZnS–SiO_2 layer with a thickness of 100 nm was initially deposited on the substrate and an inorganic resist material GSSO was then deposited over this layer by RF magnetron sputtering. In practice, this ZnS–SiO_2 layer was adopted to protect the substrate. As the GSSO layer was heated by absorbing blue light with a wavelength of 405 nm, the phase of the GSSO material was transformed from amorphous to crystalline.

A blue laser was passed through an objective lens with an *NA* of 0.65 to illuminate on GSSO film to yield nanoscale patterns, as shown in Fig. 2(a). The sample was put into an optical disk drive tester (PULSTEC ODU-1000) to be exposed. The constant linear velocity (CLV) of the sample was set to 6.61 m/s. In the tester, although contin-

* Corresponding author. Tel.: +886 3 4638800 7518; fax: +886 3 4639355.
E-mail address: eecpliu@saturn.yzu.edu.tw (C.P. Liu).

0925-8388/$ – see front matter © 2009 Elsevier B.V. All rights reserved.
doi:10.1016/j.jallcom.2009.08.075

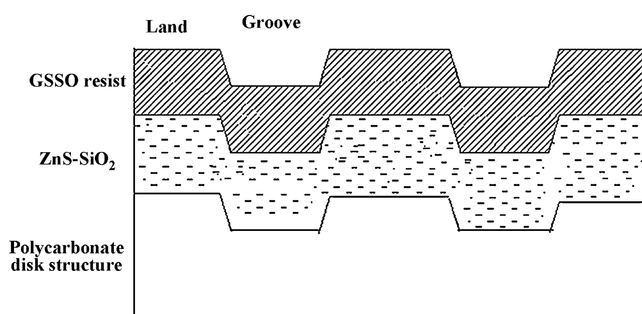

Fig. 1. Multilayer structure of our sample.

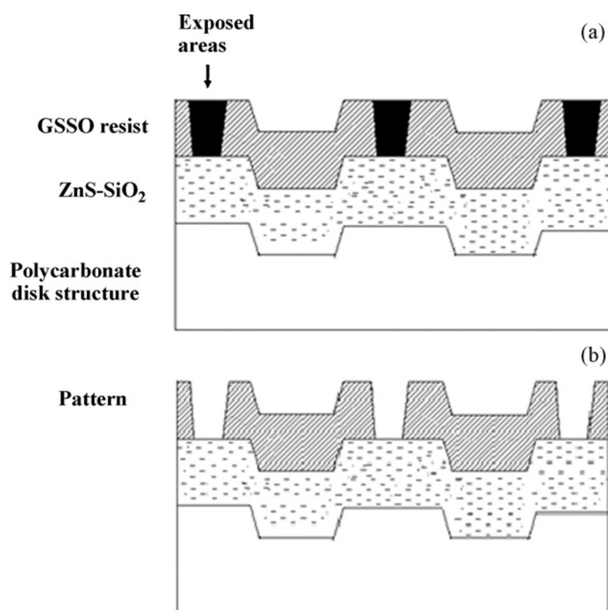

Fig. 2. Samples prepared through procedure of (a) exposure and (b) development, respectively.

uous and pulse modes of the laser can be utilized to form lines and dots, the samples that were prepared herein were adopted in continuous mode. The nanoscale pattern was obtained by developing with 0.05 M KOH solution and rinsing with de-ionized water, as shown in Fig. 2(b). The developed patterns were observed using an atomic force microscope (AFM) and a scanning electronic microscope (SEM).

2.2. Ge–Sn composition of GSSO film

To investigate the composition of Ge–Sn (GS) in GSSO film, a sample was prepared by co-sputtering with individual GSS and GS targets at different RF powers in a mixed atmosphere of Ar and O_2. The sputtering power of the GSS target was fixed for comparison, while that of the GS target was varied to yield different GS composition of GSSO film. To maintain an almost constant extinction coefficient k at 405 nm, the introduced O_2 gas-mass-flow had to be controlled. During exposure, the illuminating laser power was varied from 1.8 to 3.4 mW in steps of 0.2 mW, and each development time was 60 s. AFM revealed the variation of the pattern boundary for various samples with the same k value. Table 1 presents the sputtering parameters and development times of these samples.

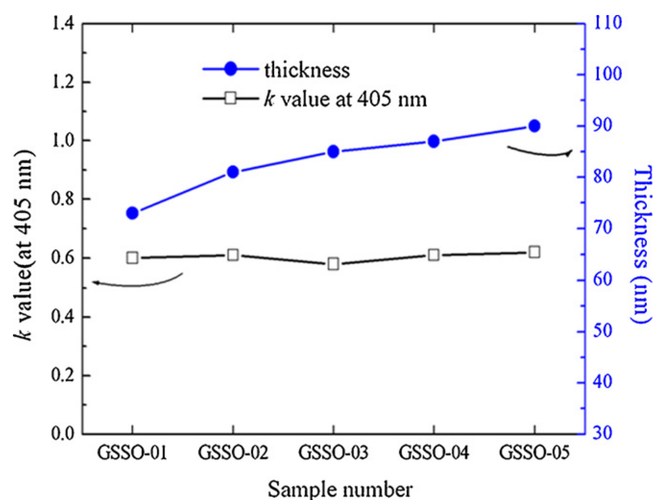

Fig. 3. GSSO film thicknesses and k values of samples GSSO-01, -02, -03, -04, and -05 were measured by ETA-optik at 405 nm.

2.3. Pattern width in GSSO film at various oxygen contents

For a given illumination power and development time, various pattern widths were obtained by controlling the oxygen content in the GSSO film at a fixed co-sputtering power. In the sputtering process, the Ar gas-mass-flow was fixed at 100 sccm while the O_2 flow was varied to control the oxygen content in the GSSO film. During exposure, the illuminating laser power was increased from 1.8 to 2.6 mW in steps of 0.1 mW, and the development time was set to 60 and 80 s. Similarly, AFM revealed variation in the pattern width for these samples.

3. Results and discussion

3.1. Composition of GS in GSSO film

The thickness and k value of the samples from GSSO-01 to GSSO-05 were measured at 405 nm using a Steag ETA-optik, as shown in Fig. 3. For comparison, the oxygen content was carefully controlled to hold the k value at 0.6, to ensure that all samples absorbed equally. Fig. 4(a)–(e) depicts the pattern boundaries of samples from GSSO-01 to GSSO-05, respectively. Fig. 5 presents the cross-sections of the GSSO-04 and GSSO-05 patterns. These two figures verify that the GSSO resist is positive. AFM topography was employed to compare directly their pattern boundaries for the same k and development time. From Fig. 4, after development, the root-mean-square (rms) of the pattern boundary of GSSO-01 was 17.7 nm, while those of GSSO-02–05 were 7–9 nm. These results demonstrate that the uniformity at the boundary was improved by increasing the GS content in the GSSO film. In Fig. 4(e), some residues are observed in the exposed region but they are not clearly shown. The cross-sections of GSSO-04 and GSSO-05 in the direction of the solid line in Fig. 4(d) and (e) clearly reveal the bottoms of the patterns, as shown in Fig. 5(a) and (b), respectively. From Fig. 5(a), the bottom of the pattern of GSSO-04 was flatter than that of GSSO-05. The residue that is displayed in Fig. 5(b) is 14 nm high, implying that the etching of GSSO-05 was incomplete after 60 s because its

Table 1
Sputtering parameters of samples with different compositions of Ge–Sn and developed times.

Sample number	Sputtering power (W)		Sputtering flow (sccm)		Sputtering time (s)	Developed time (s)
	Ge–Sb–Sn	Ge–Sn	Ar	O_2		
GSSO-01	140	0	100	30	400	60
GSSO-02	140	50	100	31	400	60
GSSO-03	140	60	100	32	400	60
GSSO-04	140	70	100	33	400	60
GSSO-05	140	80	100	34	400	60

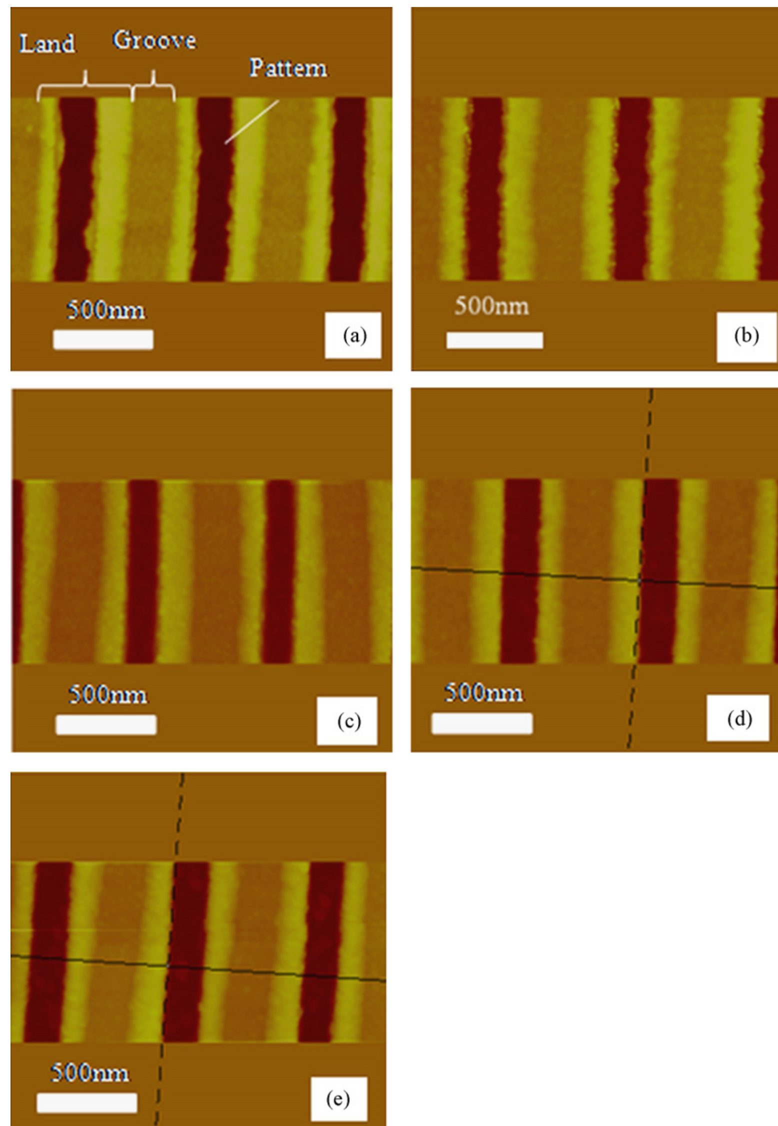

Fig. 4. The topography of pattern boundaries of (a) GSSO-01, (b) GSSO-02, (c) GSSO-03, (d) GSSO-04, and (e) GSSO-05 were observed by AFM.

rate of dissolution in the exposed region was lower than that of GSSO-04. Restated, a larger GS content in a GSSO film is associated with greater etching resistance in alkaline solution.

3.2. Dependence of pattern width on oxygen flow

Since the dissolution rate affects the pattern width, the dependence of the pattern width on oxygen flow was examined using eight samples that were prepared with four oxygen contents with two development times. These samples were designated GSSO-06 (A), GSSO-06 (B), GSSO-07 (A), GSSO-07 (B), GSSO-08 (A), GSSO-08 (B), GSSO-09 (A), and GSSO-09 (B), where (A) and (B) represent development times of 60 and 80 s, respectively. The thicknesses of the samples from GSSO-06 to GSSO-08 were all approximately 87 nm. Fig. 6 plots the dependence of the pattern width on illuminating power and Table 2 presents related parameters for these eight samples. After development, the heights of all of the developed patterns were approximately 82 nm.

Table 2
Sputtering parameters of samples at different oxygen flows and developed times.

Sample number	Sputtering power (W)		Sputtering flow (sccm)		Sputtering time (s)	Developed time (s)
	Ge–Sb–Sn	Ge–Sn	Ar	O_2		
GSSO-06 (A)	140	70	100	28	400	60
GSSO-06 (B)	140	70	100	28	400	80
GSSO-07 (A)	140	70	100	30	400	60
GSSO-07 (B)	140	70	100	30	400	80
GSSO-08 (A)	140	70	100	32	400	60
GSSO-08 (B)	140	70	100	32	400	80
GSSO-09 (A)	140	70	100	34	400	60
GSSO-09 (B)	140	70	100	34	400	80

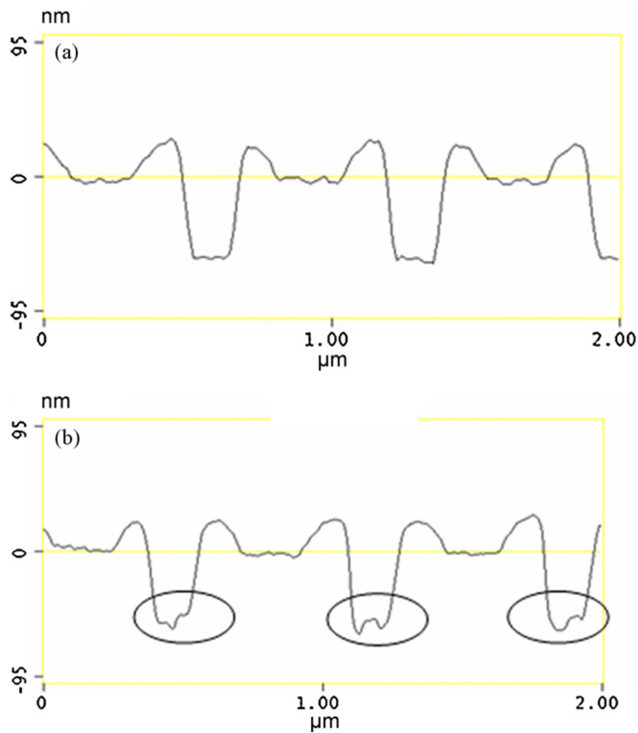

Fig. 5. The cross-sections of (a) GSSO-04 and (b) GSSO-05 were viewed along the direction of the solid line shown in Fig. 4(d) and (e).

The k values of the samples from GSSO-06 to GSSO-09 were 0.83, 0.69, 0.59, and 0.52, respectively. Table 2 and Fig. 6 demonstrate that the oxygen flows that were introduced into samples GSSO-07 (A) to GSSO-09 (A), illuminated under the same power of 2.3 mW and developed for the same period of 60 s, were 30, 32, and 34 sccm, and the widths of the samples were 195, 180, and 148 nm, respectively. A higher oxygen flow rate at a given co-sputtering power yielded a lower k value at 405 nm and a smaller line-width. The dependence of the absorption coefficient α on the extinction coefficient k is

$$\alpha = \frac{4\pi k}{\lambda} \quad (1)$$

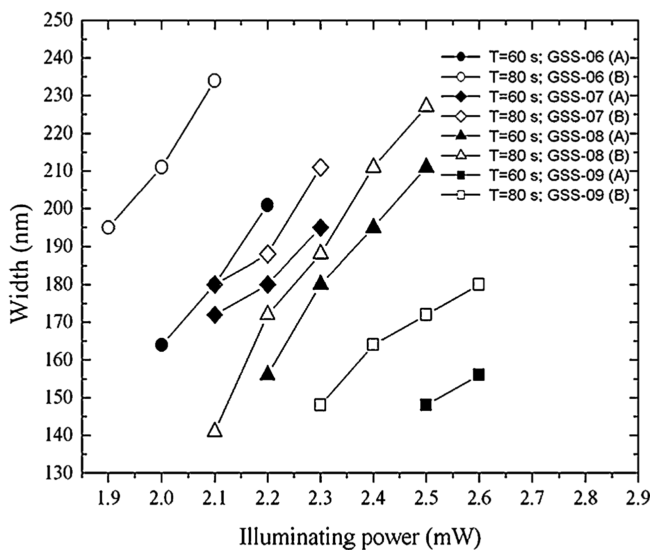

Fig. 6. The connection between the illuminating power and the pattern width was revealed.

From Eq. (1), a lower k value corresponds to lower absorption, implying that a larger oxygen content corresponds to a more transparent material and therefore a lower absorption. If the absorption coefficient of a material is lower, then the illuminating laser power required to produce the required effective temperature at the center of the focused spot is smaller [5]. This fact is consistent with the measurements plotted in Fig. 6. Higher oxygen content in a GSSO film corresponds to a lower absorption and therefore a lesser thermal diffusion, making the pattern narrower. However, the absorption of the sample must exceed a minimum threshold to enable the required patterns to be fabricated.

For samples that have been developed for a particular duration, a higher illuminating power corresponding to a larger line-width. For the GSS-08 samples in series (B) with a development time of 80 s and illuminating powers of 2.1, 2.2, 2.3, 2.4, and 2.5 mW, the corresponding widths were 141, 172, 188, 211, and 227 nm, respectively. Increasing the development times of samples illuminated with the same power yielded wider lines, as shown in Fig. 6. The pattern width of GSSO-08 (B) was approximately 140 nm—the least of the GSSO-08 series. It is much less than the diffraction limit, $\lambda/(2NA) = 320$ nm. The topography of this sample was observed by (a) AFM and (b) SEM, and shown in Fig. 7.

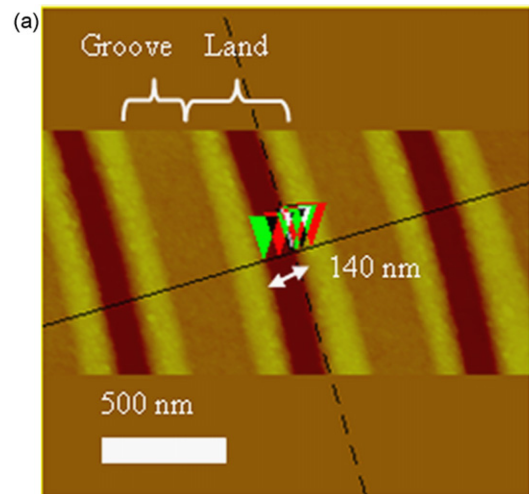

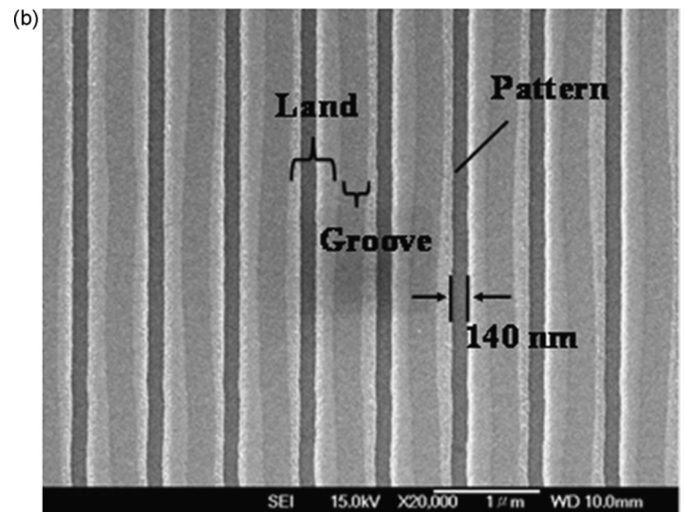

Fig. 7. The minimum pattern width of sample GSSO-08 (B) illuminated with power of 2.1 mW and developed with time of 80 s is 140 nm which can be obtained by (a) AFM and (b) SEM.

4. Conclusion

In conclusion, thermal lithography can be used more easily than optical lithography for nanoscale patterning with a width that is less than the diffraction limit. In this work, a minimum pattern width of 140 nm and a height of 82 nm fabricated on GSSO materials can be obtained by thermal lithography at a wavelength of 405 nm. Experimental data demonstrate that the inorganic GSSO resist is positive. As the GS content of a GSSO film increased, the uniformity of the pattern boundary clearly improved. However, as more GS was introduced into the GSSO film, the etching resistance in alkaline solutions increased. Therefore, the difference in dissolution rates between the exposed and unexposed states was lower.

Various absorbilities and illuminating powers were adopted to fabricate nanoscale patterns of various sizes to fulfill the future requirements of industry. In principle, the use of an exposure source with a lower wavelength for GSSO materials will yield nanoscale patterns that are narrower than 140 nm. In summary, nanoscale patterning resist by thermal lithography using an inorganic GSSO has great potential for application in industry, such as in the optical disk mastering process for ultrahigh-density optical ROM applications, and in molds.

Acknowledgment

The authors would like to thank the National Science Council of the Republic of China, Taiwan, for financially supporting this research under Contract No. NSC97-2221-E-155-037.

References

[1] M. Kuwahara, C. Mihalcea, N. Atoda, J. Tominga, H. Fuji, T. Kikukawa, Jpn. J. Appl. Phys. 61–62 (2002) 415–421.
[2] C.P. Liu, Y.X. Huang, C.C. Hsu, T.R. Jeng, J.P. Chen, IEEE Trans. Magn. 45 (2009) 2206–2208.
[3] M. Takeda, M. Furuki, T. Ishimoto, K. Kondo, M. Yamamoto, S. Kubota, Jpn. J. Appl. Phys. 39 (2000) 797–799.
[4] Y. Wada, M. Katsumura, Y. Kojima, H. Kitahara, T. Iida, Jpn. J. Appl. Phys. 40 (2001) 1653–1660.
[5] M. Kuwahara, J. Li, C. Mihalcea, N. Atoda, J. Tominga, L.P. Shi, Jpn. J. Appl. Phys. 41 (2002) L1022–1024.
[6] E. Ito, Y. Kawaguchi, M. Tomiyama, S. Abe, E. Ohno, Jpn. J. Appl. Phys. 44 (2005) 3574–3577.
[7] Y. Kawaguchi, E. Ohno, E. Ito, U.S. Patent 20050045587A1 (2005).
[8] A. Kouchiyama, K. Aratani, U.S. Patent 7175962B2 (2007).
[9] Amaya Kenji, Proc. SPIE 3676 (1999) 360–370.
[10] Meinders Erwin R., Loch Rolf A., W.O. Patent 2005101397A1 (2005).
[11] C.P. Liu, G.R. Jeng, H.E. Huang, Mater. Trans. 48 (2007) 847–853.
[12] C.P. Liu, G.R. Jeng, J. Alloys Compd. 468 (2008) 343–349.